

Effects of Preprocessing Eye Fundus Images on Appearance Based Glaucoma Classification

Jörg Meier¹, Rüdiger Bock¹, Georg Michelson², László G. Nyúl¹, and Joachim Hornegger¹

¹ Institute of Pattern Recognition, University of Erlangen-Nuremberg,
Martensstraße 3, 91058 Erlangen
{joerg.meier,ruediger.bock,laszlo.nyul,joachim.hornegger}
@informatik.uni-erlangen.de

² Department of Ophthalmology, University of Erlangen-Nuremberg,
Schwabachanlage 6, 91054 Erlangen
georg.michelson@augen.imed.uni-erlangen.de

Abstract. Early detection of glaucoma is essential for preventing one of the most common causes of blindness. Our research is focused on a novel automated classification system based on image features from fundus photographs which does not depend on structure segmentation or prior expert knowledge. Our new data driven approach that needs no manual assistance achieves an accuracy of detecting glaucomatous retina fundus images comparable to human experts. In this paper, we study image preprocessing methods to provide better input for more reliable automated glaucoma detection. We reduce disease independent variations without removing information that discriminates between images of healthy and glaucomatous eyes. In particular, nonuniform illumination is corrected, blood vessels are inpainted and the region of interest is normalized before feature extraction and subsequent classification. The effect of these steps was evaluated using principal component analysis for dimension reduction and support vector machine as classifier.

Key words: Glaucoma; Retina imaging; Digital color fundus photograph; Classification; Image enhancement

1 Introduction

Glaucoma is one of the most common causes of blindness. It is induced by the progressive loss of retinal nerve fibers in the parapapillary region. Lost fibers cannot be revitalized but the progression of the disease can be stopped [1]. For this reason, early detection of glaucoma is essential for affected patients. Diagnosis is commonly done by direct examination of the important neuroretinal rim [2] using an ophthalmoscope or based on digital retina images acquired by devices such as the Heidelberg Retina Tomograph (HRT) [3] or the Kowa NonMyd fundus camera (Fig. 1). In this work, we use the modality of color fundus photographs. The acquisition is suitable for screening applications because fundus photos can be taken very fast and without any inconvenience for patients.

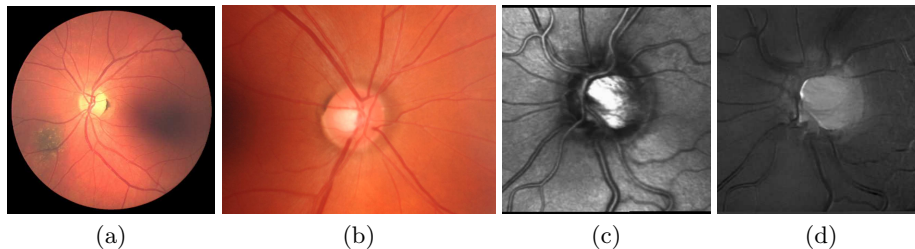


Fig. 1. Example images of the eye ground: Color fundus photographs with large (a) and small fields of view (b), HRT reflectance (c) and topographic image (d).

Existing computer aided analysis of retina images are based on segmentation which is mostly done manually or by semi-automated methods [4]. Different research groups investigate in the field of getting and selecting segmentation measurements from HRT images [5, 6]. Segmentation based techniques have one major drawback: small errors in segmentation may lead to significant change in the measurements and thus the estimation and diagnosis.

In our approach, the feature extraction and classification is fully automated and is not segmentation dependent. This appearance based approach is well-known from object and face recognition [7, 8]. It is a data driven technique based on statistical evaluation of the image data, e.g. by Principal Component Analysis (PCA). This promising approach is new in the field of retina imaging.

To provide a good basis for further investigations, we analyze the effect of normalizing the images by preprocessing methods on classification results. We show that reducing disease independent variations is possible without removing information that discriminates between healthy and glaucomatous eyes.

On one hand, nonuniform illumination is a general problem in retinal imaging. It is due to the small size of the objects and the complexity of the optic system (including both the camera and the eye) involved in the imaging process. Such inhomogeneities have to be corrected. On the other hand, blood vessels in retina images seem to be a distracting feature when diagnosing glaucoma. In our study, blood vessels are removed and those regions have to be specially treated before further processing. Additionally, a normalized input, which includes the relevant region of interest (ROI), is needed for the feature computation by appearance based approaches. Therefore, we perform localization and size normalizations before feature extraction.

2 Methods

As shown in the examples in Fig. 1, fundus images show important physiological structures of the eye ground, including the optic nerve head (ONH), the macula, and the blood vessels. Based on the usual practice in the clinic, we developed a scheme for automated processing and classification of the acquired images.

1. Correction of illumination and intensity inhomogeneities,
2. Inpainting of the blood vessels,
3. Normalization of the region of interest for diagnosis,
4. Feature extraction,
5. Classification.

The focus of the work reported here is on the preprocessing steps (1-3). These are, however, essential for providing strong features and reliable classification.

We show in this paper the effect of the preprocessing steps on glaucoma classification using a fixed configuration of feature extraction and classifier. The features are computed by PCA, and then used in a Support Vector Machine (SVM) to classify the images. The obtained results are evaluated by comparing them with given diagnoses.

2.1 Correction of Illumination and Intensity Inhomogeneity

Since the red channel of the fundus photos is often oversaturated (especially in the central, papilla region), and the blue channel is noisier, we use the green channel for processing. It shows the highest contrast between the blood vessels and the background and also for the studies of the optic nerve head. This approach is also used by other research groups [4, 9, 10]. We implemented a correction method similar to the one proposed in [9]. According to their lighting model, the observed intensity in each color channel of an image $\mathbf{F} \in \mathbb{R}^{n \times m}$ is a pixel-wise product of an illumination component \mathbf{I} and a reflectance component \mathbf{R} . The first component is due to the source illumination, while the second one is related to the structures in the retina and their properties. Taking the logarithm the pixels at (x, y) become an additive term:

$$\mathbf{F}_{\log}(x, y) = \log(\mathbf{I}(x, y) \cdot \mathbf{R}(x, y)) = \mathbf{I}_{\log}(x, y) + \mathbf{R}_{\log}(x, y). \quad (1)$$

A 4th-order polynomial surface is then fitted to model the light pattern. The surface parameters $\mathbf{p} \in \mathbb{R}^{15}$ are obtained by finding the least-squares estimate from the following (weighted) linear equation system [11]:

$$\mathbf{f}_{\log} = (\mathbf{WS})\mathbf{p}, \quad (2)$$

where \mathbf{f}_{\log} is the vector representation of \mathbf{F}_{\log} , the $\mathbf{S} \in \mathbb{R}^{N \times 15}$ matrix, where $N = n \cdot m$ is the number of pixels in the image, contains the polynomial terms of the pixel locations, and the diagonal matrix $\mathbf{W} \in \mathbb{R}^{N \times N}$ is used to mask out from the computation the structured pixels of the background and the bright ONH, which should not be used in the fitting. The diagonal elements are 1 where a pixel is considered valid for illumination estimation, and 0 elsewhere. Then, the vector of the logarithmic reflectance component \mathbf{r}_{\log} is recovered as

$$\mathbf{r}_{\log} = \mathbf{f}_{\log} - \mathbf{Sp}, \quad (3)$$

wherein the illumination artifacts and intensity inhomogeneity are considerably reduced. The reflectance component \mathbf{R} is obtained by reshaping \mathbf{r}_{\log} to matrix notation and transforming it back from logarithmic space.

2.2 Inpainting of the Vessels

Our method uses intensity information from the images as well as geometric assumptions on the width, length and structure of the vessels. We use an adaptive thresholding technique, wherein for each pixel, the median of its 15×15 neighborhood is taken as a threshold to separate foreground from background. The size of the neighborhood was determined to approximately match the size of the structures, i.e. the vessels. We create a mask by combining information from this binary mask and a Canny edge map [12]. This mask is filtered such that small objects are removed and only structures that are bounded by parallel running pairs of edges are kept. These potential vessel parts are validated by gridding and a matched filter technique [13] where edge templates are applied to the grid points at different orientations and distances. A final morphological closing of the valid regions yields the vessel mask.

The region covered by the vessel mask is inpainted. It is an iterative technique, used in photo restoration and video processing [14, 15], that interpolates missing pixel values from those of the neighborhood in a visually pleasing way. In our implementation, the vessel regions are iteratively filled layer by layer from outside inwards while the missing pixels get a weighted average of the already known neighboring values. Examples are shown in the last row of Fig. 2.

2.3 Normalization of the ONH Region of Interest

We use papilla centered fundus photos for normalization. Previously proposed registration methods map images of the same subject [16] and mostly focus on vessel structures. Meaningful registration of fundus images of different subjects, however, is problematic and may not be feasible. Thus, we only apply a circular mapping of the neuroretinal rim.

The ONH appears in fundus images as an extremely bright, mostly circular region. We used a slightly modified version of the ONH localization method of [4]. It uses a mean filtering with a large kernel and threshold probing for rough localization, and then a circular Hough transform on the edge map to find the border of the neuroretinal rim.

A square box of size three times the ONH radius, centered at the ONH center is selected as the ROI for further processing. This ROI is scaled to a fixed reference size which is needed for feature computation.

3 Evaluation

The objective of this work is to study the effect of preprocessing within the domain of automated glaucoma classification. Therefore, we evaluated different combinations of the above described methods with a fixed feature extraction technique and a fixed classifier. The ROIs were scaled (interpolated) to a fixed reference size of 128×128 pixels and that was taken directly as a high dimensional feature vector. Dimensionality reduction was done by Principal Component Analysis (PCA) [8]. We took the first 30 components as features for classification. As a classifier, we selected the ν -SVC type Support Vector Machine

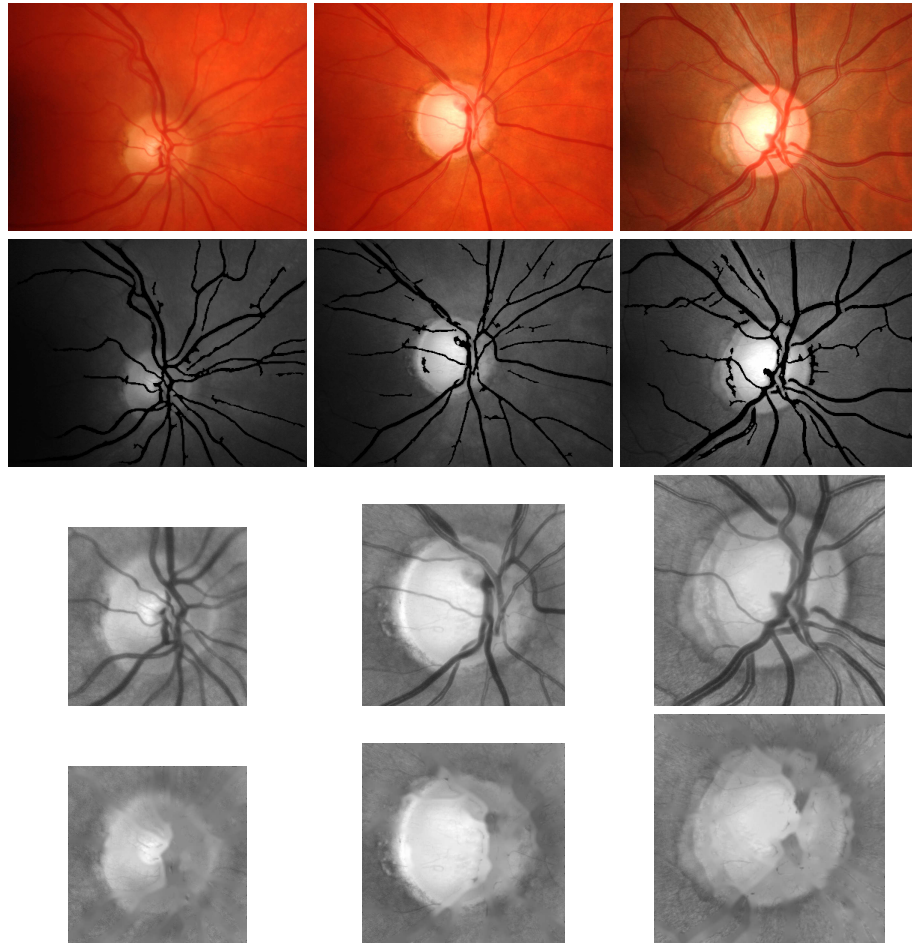


Fig. 2. Preprocessed Images, row to row: Original fundus photos, vessel masks overlaid onto the green channel image, illumination corrected and cropped ROIs, image ROIs after inpainting. First column: a healthy retina; Second column: a glaucomatous optic disc; Third column: a healthy retina with macro papilla.

(SVM) [17] with penalization parameter $\nu = 0.5$, cost-parameter $c = 1$, using the radial basis kernel and normalized input data.

The images used in this study were acquired by a Kowa NonMyd alpha digital fundus camera with a papilla centered 20° field of view and an image size of 1600×1216 pixels (see first row of Fig. 2). For evaluation, we took 200 images (50 images each of healthy and glaucomatous eyes for training and a similar mixture for separate testing; age of the subjects: 57 ± 10 years) randomly selected from the Erlangen Glaucoma Registry (EGR).

The following four combinations of the above described preprocessing steps were evaluated: with or without illumination correction and with or without vessel inpainting (see Table 1). The normalization of the ONH region of interest is performed in all cases.

Table 1. Configurations of preprocessing steps and results of glaucoma classification.

method		N	VN	IN	IVN
Preprocessing	Illumination correction			•	•
	Vessel inpainting		•		•
	ROI normalization	•	•	•	•
Classification	Success rate (testing data)	79 %	77 %	79 %	81 %
	F-measure Healthy	81 %	79 %	80 %	84 %
	F-measure Glaucoma	76 %	75 %	78 %	78 %

4 Results

The success rate and the F-measures of the four cases in Table 1 are indicators for the discriminative power regarding glaucoma. The rather consistent success rate varies from 77% to 81%. The detection of healthy subjects (F-measure between 79% and 84%) works slightly better than the detection of glaucomatous case (F-measure between 75% and 78%). Although the images contain illumination inhomogeneity and/or varying vessel branches (methods N, VN, IN), the very similar success rates show that PCA generates reasonable features.

When illumination correction or vessel exclusion is applied (method VN, IN), there is only a small variation (around 2%) in the success rate and F-measures compared to the non-corrected images (method N). This indicates that no discriminative information between healthy and glaucomatous cases is lost. If we apply both methods (method IVN), we can even slightly increase the classification performance (81%) when looking at the pixel values with PCA. According to [6], human observers looking at fundus images reach a F-measure for glaucoma of 79% (average of 3 doctors each examining 89 images). Our system which does not require any manual user interaction gains almost the same number (78%).

The preprocessing, especially the ROI normalization which is done in all cases, allows a robust data driven classification. However, we expect more benefit from the illumination corrected and vessel inpainted images when considering more sophisticated image-based features, like textures or frequency coefficients. Finding more suitable features and evaluating other classifiers is the subject of our ongoing work.

5 Conclusion

We presented our data driven classification system which is new in the field of retina imaging. Instead of previous studies, we do not rely on segmentation results or expert knowledge as features and no user interaction is necessary in the process. In particular, we evaluated methods for preprocessing color retina images. They correct and normalize variations in the image data that do not correspond to the disease. Nonuniform illumination is corrected, blood vessels are eliminated, and the region of interest is normalized before feature extraction.

The outcome of the image processing is twofold. First, we showed that adequate and disease dependent preprocessing allows an automated appearance based classification compareable to human observers. To our knowledge there are no other (semi-) automated methods to diagnose glaucoma on fundus images. The (still simple) PCA method provides already a classification success rate of 81%. The normalized images are a basis for future feature extraction methods which will be integrated in the flexible system architecture. Second, our clinical partners regard the generated images, such as “vessel-free” retina photos or PCA eigenimages, as useful additional information which will (hopefully) be used in visual assessments as well. Physicians can use these images to support their diagnosis and gain insight into retinal changes of the disease.

Acknowledgment

The images and diagnoses used in this study were obtained from the Erlangen Glaucoma Registry. The work of R. Bock was supported by the SFB 539 subproject A4, sponsored by the German Research Foundation. The work of J. Meier was supported by a scholarship from the International Max Planck Research School. The work of L.G. Nyúl was supported by a research fellowship from the Alexander von Humboldt-Foundation.

References

1. Sivalingam, E.: Glaucoma: An overview. *J Ophthalmic Nurs Tech* **15**(1) (1996) 15–18
2. Lester, M., Garway-Heath, D., Lemij, H.: *Optic Nerve Head and Retinal Nerve Fibre Analysis*. European Glaucoma Society (2005)
3. Malinovsky, V.E.: An overview of the Heidelberg Retina Tomograph. *J Am Optom Assoc* **67**(8) (1996) 457–467

4. Chrástek, R., Wolf, M., Donath, K., Niemann, H., Paulus, D., Hothorn, T., Lausen, B., Lämmer, R., Mardin, C., Michelson, G.: Automated segmentation of the optic nerve head for diagnosis of glaucoma. *Med Image Anal* **9**(4) (2005) 297–314
5. Swindale, N.V., Stjepanovic, G., Chin, A., Mikelberg, F.S.: Automated analysis of normal and glaucomatous optic nerve head topography images. *Investig Ophthalmol Vis Sci* **41**(7) (2000) 1730–1742
6. Greaney, M.J., Hoffman, D.C., Garway-Heath, D.F., Nakla, M., Coleman, A.L., Caprioli, J.: Comparison of optic nerve imaging methods to distinguish normal eyes from those with glaucoma. *Invest Ophthalmol Vis Sci* **43**(1) (2002) 140–145
7. Hornegger, J., Niemann, H., Risack, R.: Appearance-based object recognition using optimal feature transforms. *Pattern Recogn* **2**(33) (2000) 209–224
8. Zhao, W., Chellappa, R., Phillips, P.J., Rosenfeld, A.: Face recognition: A literature survey. *ACM Comput Surv* **35**(4) (2003) 399–458
9. Narasimha-Iyer, H., Can, A., Roysam, B., Stewart, C.V., Tanenbaum, H.L., Majerovics, A., Singh, H.: Robust detection and classification of longitudinal changes in color retinal fundus images for monitoring diabetic retinopathy. *IEEE Trans Biomed Eng* **53**(6) (2006) 1084–1098
10. Hoover, A., Kouznetsova, V., Goldbaum, M.: Locating blood vessels in retinal images by piecewise threshold probing of a matched filter response. *IEEE Trans Med Imag* **19**(3) (2000) 203–210
11. Walter, T., Klein, J.C.: Automatic detection of microaneurysms in color fundus images of the human retina by means of the bounding box closing. In: Proceedings of the Third International Symposium on Medical Data Analysis, ISMDA 2002, Rome, Italy. Volume 2526 of *Lect Notes Comput Sci.* (2002) 210–220
12. Canny, J.F.: A computational approach to edge detection. *IEEE Trans Pattern Anal Mach Intell* **8**(6) (1986) 679–698
13. Can, A., Shen, H., Turner, J.N., Tanenbaum, H.L., Roysam, B.: Rapid automated tracing and feature extraction from retinal fundus images using direct exploratory algorithms. *IEEE Trans Inform Tech Biomed* **3**(2) (1999) 125–138
14. Bertalmio, M., Sapiro, G., Caselles, V., Ballester, C.: Image inpainting. In: Proceedings of the 27th annual conference on Computer graphics and interactive techniques, SIGGRAPH 2000, New Orleans, USA. (2000) 417–424
15. Shen, J., Chan, T.F.: Mathematical models for local nontexture inpaintings. *SIAM J Appl Math* **62**(3) (2002) 1019–1043
16. Karali, E., Asvestas, P., Nikita, K.S., Matsopoulos, G.K.: Comparison of different global and local automatic registration schemes: An application to retinal images. In: Proceedings of Medical Image Computing and Computer-Assisted Intervention, MICCAI 2004, Saint-Malo, France. Volume 3216 of *Lect Notes Comput Sci.* (2004) 813–820
17. EL-Manzalawy, Y., Honavar, V.: WLSVM: Integrating LibSVM into Weka Environment. (2005) Software available at <http://www.cs.iastate.edu/~yasser/wlsvm>.